# Scanning Cytometry with a LEAP: Laser-Enabled Analysis and Processing of Live Cells In Situ

Peter Szaniszlo,[1] William A. Rose,[1] Nan Wang,[2] Lisa M. Reece,[3,4] Tamara V. Tsulaia,[5] Elie G. Hanania,[6] Cornelis J. Elferink,[5] and James F. Leary[3,4,7]*

[1]Department of Microbiology and Immunology, University of Texas Medical Branch at Galveston, Galveston, Texas
[2]Department of Pathology, University of Texas Medical Branch at Galveston, Galveston, Texas
[3]Department of Basic Medical Sciences, School of Veterinary Medicine, Purdue University, West Lafayette, Indiana
[4]Bindley Biosciences Center at Discovery Park, Purdue University, West Lafayette, Indiana
[5]Department of Pharmacology and Toxicology, University of Texas Medical Branch at Galveston, Galveston, Texas
[6]Cyntellect, Inc., San Diego, California
[7]Department of Biomedical Engineering, Weldon School of Biomedical Engineering, Purdue University, West Lafayette, Indiana

**Background:** Scanning cytometry now has many of the features (and power) of multiparameter flow cytometry while keeping its own advantages as an imaging technology. Modern instruments combine capabilities of scanning cytometry with the ability to manipulate cells. A new technology, called LEAP™ (laser-enabled analysis and processing), offers a unique combination of capabilities in cell purification and selective macromolecule delivery (optoinjection).

**Methods:** LEAP-mediated cell purification and optoinjection effects were assessed in model experiments using adherent and suspension cell types and cell mixtures plated and processed at different densities. Optoinjection effects were visualized by delivering fluorescent dextrans into cells. Results were analyzed using the LEAP instrument's own imaging system as well as by fluorescence and confocal microscopy.

**Results:** Live cell samples (adherent and suspension) could be purified to 90–100% purity with 50–90% yield, causing minimal cell damage depending on the cell type and plating density. Nearly one hundred percent of the targeted cells of all cell types examined could be successfully optoinjected with dextrans of 3–70 kDa, causing no visual damage to the cells. Indirect optoinjection effects were observed on untargeted cells within 5–60 μm to targeted areas under conditions used here.

**Conclusions:** LEAP provides solutions in cell purification and targeted macromolecule delivery for traditional and challenging applications where other methods fall short. © 2006 International Society for Analytical Cytology

**Key terms:** cytometry; scanning cytometry; fluorescence microscopy; single cell analysis; cell purification; selective ablation; laser-optoinjection; selective delivery; tissue surgery

While scanning cytometry has been with us for many years, the modern era of scanning cytometry began with the pioneering efforts of Kamentsky and others to produce a user-friendly commercial version through Compu-Cyte, as recently reviewed by Kamentsky (1) and Luther et al. (2). Importantly, the new generation of instruments has the capability of fluorescence-based measurements that make use of the rich diversity of molecular probes now available. These molecular probes can bear different color fluorescent tags, which can then be combined in Boolean combinations to distinguish cell subpopulations; much as has been done with flow cytometry (3). While excellent work was done extracting features from Feulgen and other nonfluorescent stains, one could only extract information that was there. Application of multi-color molecular probes greatly adds to the information content of each image pixel, essentially extending the analysis from two-dimensional to multidimensional. The result of these advances is that scanning cytometry now has many of the features (and power) of multiparameter flow cytometry while keeping its own advantages as an imaging technology. These advantages of scanning cytometry include the ability to the following: (a) perform fluorescence and light scatter imaging measurements on either attached or suspension cells with a minimum of cell

manipulation, (b) measure not only cell and nuclear morphology but also the spatial distribution of fluorescent molecular probes, and (c) return to the same spatial location for additional measurements of the same probes in time (kinetic measurements) or for restaining with different probes. Other sophisticated imaging instruments with capabilities for high-throughput screening have been developed (4,5) and sold by Beckman-Coulter (4) and Cellomics (6). A wide variety of image cytometry applications have been developed by several key laboratories (7–16).

More recently, instruments have been developed that combine some of the capabilities of scanning cytometry with the ability to manipulate cells. One of these, laser capture microdissection (LCM) was developed by researchers at the National Cancer Institute (17) and is now marketed through Arcturus. This is widely used by hundreds of research laboratories around the world and while a powerful technology, it has the technical limitation that the cells be either fixed or frozen. LCM has been an important tool in the new field of microgenomics, which purifies cell subpopulations prior to gene array analyses. Measurements, however, cannot be made in a conventional aqueous environment. Another technology of "laser pressure catapulting" has been developed by PALM Microlaser Technologies AG, now a wholly owned subsidiary of Carl Zeiss AG in Germany, to handle this problem. Another instrument has the ability to manipulate single cells with laser tweezer technology (18) and is now commercially available through Cell Robotics. A reliable technique, manual microinjection, is an extremely tedious process, requiring both skill and patience. Even more recent automated microinjection techniques by Eppendorf AG in Germany, while representing an important advance, still cause considerable cell injury and are still comparatively slow (hundreds of cells/hour) in terms of providing large numbers of microinjected cells.

In this article, we describe a new technology, called LEAP (Laser Enabled Analysis and Processing), developed by Cyntellect (19–22) that we have been beta-testing in our laboratory. LEAP technology provides many of the advantages of LCM and laser catapulting, as well as the ability to manipulate single cells by a variation of laser tweezer technology; LEAP provides a method of live cell sorting based on laser ablation. Unlike these other technologies, the LEAP instrument provides a convenient method for high-speed microinjection of macromolecules into living cells using a pulsed laser ("laser optoinjection") set at sublethal energies. This optoinjection is very fast (hundreds of cells/s) and, unlike electroporation, has a very low rate of injury to cells, which can be individually selected on the basis of multiple fluorescent probes in an automated molecular imaging process. LEAP can be performed in a totally sealed environment in a process akin to inverted fluorescence microscopy with long-working length distance objectives. It also offers a new method of sorting or optoinjecting cells under sterile conditions and provides a safe means of handling biohazardous cells and agents.

## MATERIALS AND METHODS
### Cell Cultures

**CEM.** Human, CD4+ T-cell line (acute lymphoblastoid leukemia) obtained through the AIDS Research and Reference Reagent Program, Division of AIDS, NIAID, NIH. CEM cells were cultured using RPMI 1640 medium with 2mM L-glutamine and 10% fetal bovine serum in the presence of 5% $CO_2$ at 37°C.

**KG-1a.** Human, CD34+ stem-cell cell line (human bone marrow acute myelogenous leukemia, ATCC Cat. No. CCL-246.1) was kindly provided by Dr. Brian R. Davis. KG-1a cells were cultured using Iscove's modified Dulbecco's medium with 4 mM L-glutamine and 20% fetal bovine serum in the presence of 5% $CO_2$ at 37°C.

**HeLa.** Human, epithelial cell line (cervix adenocarcinoma) was kindly provided by Dr. Kui Li (Department of Microbiology and Immunology, University of Texas Medical Branch, Galveston, TX). HeLa cells were cultured using Eagle minimum essential medium with 2 mM L-glutamine and 10% fetal bovine serum in the presence of 5% $CO_2$ at 37°C.

RPMI 1640 medium, Iscove's modified Dulbecco's medium, Eagle minimum essential medium, fetal bovine serum, trypsin, and glutamine were purchased from Invitrogen (Carlsbad, CA).

**Hepatocytes.** Mouse primary hepatocytes were isolated by the collagenase perfusion from either wild-type C57Bl/6 mice (The Jackson Lab, Bar Harbor, ME) as described previously (23). Hepatocytes were cultured in Attachment media consisted of Williams E (Sigma, St. Louis, MO), 5% Fetal bovine Serum (Hyclone, Logan, UT), 1% Penicillin/Streptomycin (Invitrogen, Carlsbad, CA), and 100 nM Insulin (Invitrogen, Carlsbad, CA). After the 4 h of incubation, cells were plated in Growth media consisted of Williams E, 1% Streptomycin/Streptomycin, 100 nM Insulin, and 2 ng/mL endothelial growth factor (Invitrogen, Carlsbad, CA).

For the experimental purposes, liver cells were plated on plastic 6-well plates (Corning, Acton, MA). Cell density ranged from $1 \times 10^5$ to $1 \times 10^6$/per well. During the 4-h attachment period, cells were infected with the adenovirus AdGFP (24) at a multiplicity of infection of 100 (based on infection of 293 cells), resulting in infection of about 50% of the hepatocytes. Cells were supplemented with growth medium following attachment, and were either maintained overnight at 37°C in a 5% $CO_2$ humidified incubator, or were immediately stained with CellTracker Orange (CTO; Invitrogen, Carlsbad, CA) for LEAP experiments.

### Cell Preparation for LEAP Processing

**HeLa cells.** HeLa cells were trypsinized and plated to confluency in a Lab-Tek® II Chamber Slide™ System 8 Well Glass Slide (Nalge Nunc, Naperville, IL) using HeLa culture medium. Cells were incubated overnight in the presence of 5% $CO_2$ at 37°C. For ablation experiments, the cells were washed once with serum-free 199 medium (Invitrogen, Carlsbad, CA) and

left in serum-free 199 medium. For optoinjection experiments, the cells were washed once with serum-free 199 medium, then the medium was changed to serum-free 199 medium that contained Tetramethylrhodamine (TMR)-conjugated dextrans of $M_W$ = 3, 10, 40, or 70 kDa (Invitrogen, Carlsbad, CA) at a concentration of 100 μg/mL.

**Hepatocytes.** Primary hepatocyte cultures comprising 50% adenoviral infection (GFP positive cells) were washed once and maintained in serum-free 199 medium in the original 6-well tissue culture plate (Corning, Acton, MA) for LEAP. Following LEAP, cells were returned to Growth media for subsequent incubation and analysis.

**Model cell mixtures.** CEM and KG-1a cells were counted and tested for viability using Trypan blue (Invitrogen, Carlsbad, CA) exclusion. CEM cells ($3.0 \times 10^6$) were labeled with phycoerythrin (PE)-conjugated, murine, anti-CD4 antibody (Caltag Laboratories, Burlingame, CA) using factory recommended protocols. KG-1a cells ($3.0 \times 10^6$) were labeled with FITC-conjugated, murine, and anti-CD34 antibody (Caltag Laboratories, Burlingame, CA) using factory recommended protocols. Labeled KG-1a and CEM cells were pelleted and resuspended separately in serum-free 199 medium. Both cell suspensions were recounted and appropriate volumes of each cell type for a 50% mixture were calculated. The 50% cell mixture was then prepared according to the calculations and plated at different densities in a Lab-Tek® II Chamber Slide™ System 8 Well Glass Slide. The plated slide was centrifuged at 400g for 10 min using an ALC PM140 centrifuge (ALC, Winchester, VA).

**KG-1a cells.** For optoinjection KG-1a cells were washed once with serum-free 199 medium, then they were resuspended in serum-free 199 medium that contained TMR-conjugated dextrans of $M_W$ = 3, 10, 40, or 70 kDa at a concentration of 100 μg/mL. The cells were plated in this dextran-containing medium at high density in a Lab-Tek® II Chamber Slide™ System 8 Well Glass Slide. The plated slide was centrifuged at 400g for 10 min.

## LEAP Instrument

The Laser Enabled Analysis and Processing (LEAP) instrument platform has been previously described by Koller et al (21). Briefly, a Q-switched, diode-pumped, solid-state, Nd:YAG laser (JDS Uniphase, San Jose, CA) was coupled with a novel, custom designed fluorescence imaging system (22). The average power output of this laser at 532 nm is about 30 mW. It pulses at a 2 kHz frequency with a pulse width of 0.5 ns, and peak power output of above 30 kW at 532 nm. The instrument was designed with an achromatic F-theta lens that when combined with high-speed galvanometer mirrors, allows for large surface area imaging without the need to move the stage for every view. Brightfield imaging is provided by light-emitting diodes, and epifluorescence excitation is provided by a halide/xenon hybrid lamp, both of which are viewed utilizing two mega-pixel-γ-intensified CCD cameras. Custom software is used to direct the laser beam pulses at targets that can be user-selected or auto-selected by the custom software.

## LEAP-Mediated Cell Purification

Samples were loaded into the LEAP instrument via the sample-loading platform using the sample loading software. A small section of the bottom right corner of each well was used for empirically determining the proper laser settings for ablation or cell removal. The position of the beam waist of the laser was adjusted by changing the beam expander (BE) settings so that it was in the optimal position for ablation/cell removal for the given experiment. Similarly, the optimal laser power was adjusted using the LEAP neutral density filter (NDF). The optimal laser power was found when targeted cells in the calibration area were destroyed or moved from their original position, but untargeted cells were not affected. The optimal number of pulses and repeats was determined in earlier experiments and used here. For these experiments, a BE position of 0.6–1.0 (arbitrary units), NDF position 100–200 (arbitrary units), 1–5 pulses, and 1–3 repeats were determined to be the best conditions.

## LEAP-Mediated Optoinjection

The same method was used as described for cell purification with the following modifications: once the optimal BE position was determined, the NDF setting was adjusted to decrease the laser power until no cell damage could be observed. The optimal conditions for these experiments were found to be a BE position of 0.8–1.0, NDF position 200–240, 1–5 pulses, 1–3 repeats, with a 4-s delay between repeats.

## Analysis of Results

After processing on LEAP, the cells were washed three times with the appropriate media for the cell type. In the ablation and optoinjection experiments of HeLa cells, samples were viewed utilizing a custom Diaphot Inverted Fluorescent Microscope (Nikon, Garden City, NY) and photographs were taken with a CoolPIX 990 Digital Camera (Nikon, Melville, NY). Dextran-containing HeLa cells were visualized using a custom microscope fluorescent filter setup for TMR (excitation: 525 nm/dichroic: 570 nm/emission 605 nm). In the ablation/purification experiments of hepatocytes and the KG-1a/CEM cell mixtures, the samples were visualized, pictures were taken, and images of the same view were overlayed using the LEAP instrument's optics, cameras, and image analysis software. PE-, FITC-, CTO-, and GFP-labeled cells were visualized using manufacturer recommended LEAP filter configurations. Single channel overlay images that were used to monitor cell movement due to LEAP-shooting were recolored using Paintshop Pro 6.00 (Jasc Software, Minneapolis, MN). Confocal images of optoinjected KG-1a cells were viewed and photographed using a Zeiss LSM 510 UV-

META confocal imaging system. (Carl Zeiss, Oberkochen, Germany).

## RESULTS
### Ablation and Purification of Live Adherent Cells

Figure 1 describes a set of experiments designed to explore the power and versatility of the LEAP platform for cell purification. For the first experiment, an initial model cell culture of HeLa cells was plated in a semiconfluent monolayer and processed live by LEAP. Defined, easily recognizable geometrical regions of the cell monolayer were LEAP-ablated using the grid-pattern shooting method (Fig. 1A). To assess LEAP-related effects, targeted regions, their immediate surrounding areas, and the rest of the culture were monitored for ablation/cell damage and compared with control cultures. After optimizing the shooting conditions, virtually 100% of the targeted cells were completely ablated, with only a very few unattached, dead/damaged cells found in the targeted areas. The targeted regions could be very accurately ablated with sharp edges and angles circumscribing the ablated area. Indeed, targeted regions could also be ablated at any desired configuration (Fig. 1A, Panels 1–4). A few damaged cells were observed within a 1–2 cell diameter range (5–20 μm) from the targeted area (Panel 1, Region 1). The rest of the cells throughout the culture did not show any signs of damage. Most of the cells bordering the ablated region (Panel 1, Region 2) and the cells plated towards the periphery of the slide chamber (Panel 1, Region 3) appeared to be unaffected. For this ablation application, high laser power (50–100%) with very few (1–3) repeats was found to be the most efficient.

After establishing the basic characteristics of LEAP-mediated cell ablation, we modeled the more life-like problem of purifying a cell culture from contaminating individual cells. Purification of a confluent/semiconfluent monolayer of unlabeled HeLa cells from a small subset of doped-in contaminating labeled HeLa cells (below 5%) could be achieved by targeting these unwanted cells individually, using the shooting conditions described. The ablating/damaging LEAP-effect on the untargeted neighboring cells caused a 10–20% loss in the purified unlabeled HeLa cell population. This approach resulted in virtually 100% purity with above 80% yield (data not shown).

To purify a cell mixture with above 5% unwanted cell ratio, a lower cell density culture was needed to avoid significant cell loss by LEAP-purification. The optimal plating density had to be determined empirically based on the contaminating cell ratio and the fragility/sensitivity of the given cell type to LEAP-irradiation. Figure 1B demonstrates an example of a highly LEAP-sensitive, adherent cell type with 50% contaminating cell ratio. In this experiment, freshly isolated hepatocytes were infected with an Adenovirus expressing the green fluorescent protein (GFP) reporter gene at ~50% infection efficiency. The GFP expressing cells were subsequently LEAP-purified for further experiments. These conditions required low-density cell plating of single cells, with the cells being 2–5 cell dia-

meters (30–100 μm) apart. The culture was briefly treated with CTO to label all cells for targeting. For visualization in the instrument, which produces grey-level images on each of its two cameras, the fluorescence is shown in pseudo-colors that map GFP (green) and CTO (orange).

Figure 1B (Panel 1) shows a simple two-color fluorescent image of hepatocytes taken by LEAP before laser processing. GFP-expressing cells appear green to yellow depending on the relative strength of their green and orange fluorescence, while GFP-negative cells appear orange. We targeted these negative cells using the laser and another two-color image was created of the same field-of-view immediately after the shooting was performed (Fig. 1B, Panel 2). Hepatocytes have the tendency to form multicellular conglomerates (Panels 1–4, Regions 1) that may contain positive and negative cells at the same time. These cell clusters were not targeted because LEAP-processing was found to have an all-or-nothing effect on them where targeting any one of these cells detached the entire cluster. The rest of the GFP negative cells were all ablated (Panels 1, 2, Regions 2, 3) or seriously damaged (Panels 1, 2, Region 4).

For this sensitive cell type, maintaining attachment to the plate surface is crucial. Detached hepatocytes are much more likely to die by apoptosis than to reattach. To monitor the exact position of each individual cell before and after LEAP-shooting, we superimposed the before and after images of each view. Figure 1B (Panel 3) was created by overlaying the green fluorescent images of the same view before (green) and after (black) the shooting. Only GFP-positive cells are visible on this image, since the negative cells do not emit light at this wavelength (525 nm). Black spots on top of green spots represent GFP-positive cells that have not been moved by LEAP processing (Panel 3, Region 1). An exposed green spot represents a GFP-positive cell that has moved away from that position during the shooting while a black spot alone represents the new position of a moved GFP-positive cell (Panel 3, Region 2). The vast majority of GFP-positive cells were found to be unaffected. Similarly, Figure 1B (Panel 4) was created by overlaying the orange fluorescent images of the same view before (orange) and after (black) LEAP processing. Since all cells are CTO-positive, both GFP-positive and -negative cells are visible in this image. Cells that are visible in this image, but not in the previous image, are the GFP-negative cells (Panel 4, Regions 2, 3, 4). Orange-only spots represent removed cells (Panel 4, Regions 2, 3), while small gray spots appeared on top of larger orange spots when the shooting resulted in seriously damaged cells or cell debris (Panel 4, Region 4). Taken together, Figure 1B (Panels 3 and 4) revealed that most of the GFP-negative cells had been removed by LEAP purification while most GFP-positive cells remained intact. This purification method resulted in above 90% cell recovery with ~90% purity. The remaining GFP-positive cells suffered no apparent damage and could be cultured further. For this application, medium-level laser power (25–75%) with several (5–15) repeats proved to be the most efficient.
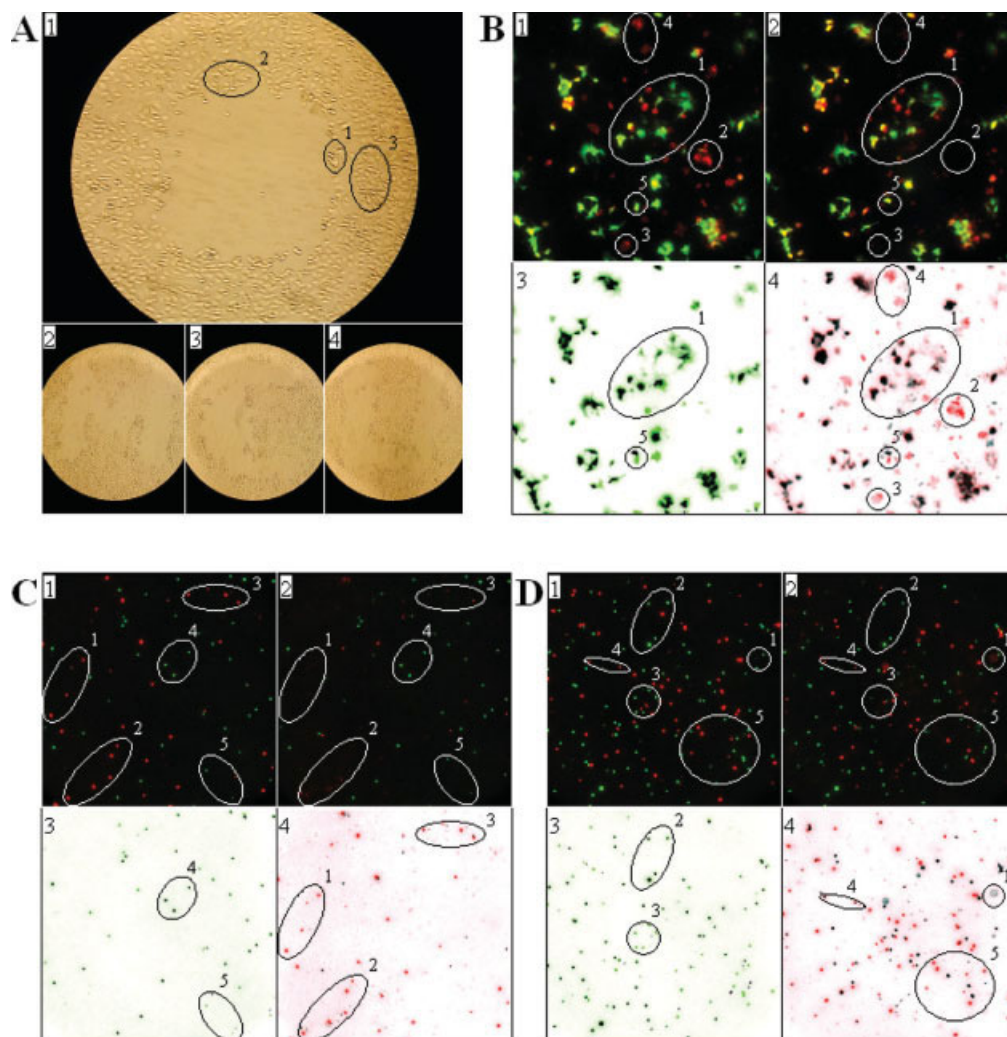
FIG. 1. Applications of LEAP-mediated cell purification. **A:** Ablation of regions with different geometrical shapes (Panel 1, square; Panel 2, M; Panel 3, C; and Panel 4, U) from confluent HeLa monolayer (MCU, molecular cytometry unit). The ablation process damaged very few cells (region 1), while most of the remaining cells were unaffected (regions 2 and 3). The ablated areas very accurately follow the shooting pattern. **B:** Purification of GFP expressing hepatocytes. GFP and CTO images of the same view were overlaid to show GFP negative cells (orange) and GFP-expressing cells with GFP positive (green-yellow) and negative (orange) portions, Panel 1, GFP/CTO before; Panel 2, GFP/CTO after; Panel 3, GFP images before purification (green) and after (black) overlaid; and Panel 4, CTO images before purification (orange) and after (black) overlaid. Most GFP negative cells (only orange) were ablated (region 2), fragmented (region 3), or detached (region 4) while most GFP expressing cells (green-yellow-orange) were unaffected (region 1). Very few GFP positive cells were detached (region 5). **C:** Purification of suspension cells-low density. CD34-FITC labeled KG-1a cells (green) and CD4-PE labeled CEM cells (orange) were mixed then KG-1a cells were purified by LEAP ablation/detachment of the CEM cells, Panel 1, KG-1a/CEM before; Panel 2, KG-1a/CEM after; Panel 3, KG-1a cells before/after (green/black); and Panel 4, CEM cells before/after (orange/black). All CEM cells have been ablated (region 1) or detached (regions 2 and 3) while most KG-1a cells remain unaffected (region 4). Very few KG-1a cells were moved (region 5). **D:** Purification of suspension cells-high density. KG-1a cells (green) and CEM cells (orange) were mixed then KG-1a cells were purified by LEAP ablation/detachment, Panel 1, KG-1a/CEM before; Panel 2, KG-1a/CEM after; Panel 3, KG-1a cells before/after (green/black); and Panel 4,. CEM cells before/after (orange/black). Most CEM cells have been detached (regions 1 and 5) but some were not affected (region 4). Although some KG-1a cells have been moved (region 3), most KG-1a cells were unaffected (region 2).

## Purification of Live Suspension Cells

As a model cell mixture for suspension cells, a 50% mix of differentially labeled KG-1a cells (CD34-FITC label) and CEM cells (CD4-PE label) was prepared. The mixture was plated at different cell densities in 8-chambered slides and the slides were gently centrifuged to settle all cells on the slide surface in a semiattached state. Figure 1C illustrates purification results after low-density plating with the cells being 5–10 cell diameters (30–100 µm) apart. Figure 1C (Panel 1) is a two-color fluorescent image of the cells taken

by the LEAP instrument prior to laser processing. KG-1a cells appear green; CEM cells are orange. We targeted orange (PE-positive) cells with the laser and a subsequent two-color image was created of the same view after the shooting (Fig. 1C, Panel 2). Most CEM cells disappeared (i.e. were ablated or detached and floated away) from the field-of-view (compare Panels 1 and 2, Regions 1, of both images). The rest of the CEM cells were moved from their original location (Panels 1 and 2, Regions 2, 3); many of these detached cells appeared obviously damaged. Figure 1C (Panel 3) was

Table 1
*LEAP-Mediated Purification of Adherent and Suspension Cells*

|  | Purity (%) | Yield (%) | Damage (%) | Laser power (%) |
|---|---|---|---|---|
| Adherent cells–confluent (region)[a] | 100 | 90 | Some | 50–100 |
| Adherent cells–confluent (individual up to 5%) | 100 | 80 | Some | 50–100 |
| Adherent cells–low density (Individual) | 90 | 90 | Some | 25–75 |
| Suspension cells–high density (individual) | 90–95 | 50–75 | None | 25–50 |
| Suspension cells–low density (individual) | 95–100 | 80 | None | 25–75 |

[a]Ablating defined regions from a confluent monolayer of cells. All other rows describe purification of cell samples from individual contaminating cells.

created by overlaying the green fluorescent images of the same view before (green) and after (black) the shooting of the cells. This image exhibits only the KG-1a cells, and confirms that the majority of them remained attached (Region 4) with only a few of them moved (Region 5). Figure 1C (Panel D) was created by overlaying the orange fluorescent images of the same view before (orange) and after (black) LEAP processing. Only CEM cells are visible here, confirming that virtually none of the targeted CEM cells remained attached (Panel 4, Regions 1–3). This purification method resulted in greater than 80% cell recovery with 95–100% purity. The recovered, purified KG-1a cells suffered no apparent damage and could be cultured further. For this application, medium-level laser power (25–75%) using a few (1–5) repeats was preferred.

Figure 1D exhibits purification results of the same 50% KG-1a/CEM cell mixture after higher-density cell seeding with the cells being 1–5 cell diameters (10–50 μm) apart. Figure 1D (Panel 1) is a two-color fluorescent image of the cells taken by the LEAP instrument before laser processing. In the mixture of KG-1a (green) and CEM cells (orange), the LEAP software was used to target and eliminate the latter. Another two-color image was created of the same field-of-view after shooting (Fig. 1D, Panel 2). Since this plating density only allowed lower power LEAP shooting to preserve untargeted KG-1a cells, significantly fewer targeted cells had completely disappeared from the view after shooting than with low density plating. Some targeted cells could be observed to be floating above the focal plane of LEAP's CCD camera (Panel 2, Region 1). Figure 1D (Panel 3) was created by the same overlay technique used in the earlier images, where green areas and black spots represent FITC-labeled cells before and after laser shooting, respectively. Only KG-1a cells are visible and there is visual confirmation that a good portion of them remains attached (Panel C, Region 2). It should be noted that a significant number of KG-1a cells were found to have moved away from their origins by the indirect effects of the LEAP shooting (Panel C, Region 3). Figure 1D (Panel 4) was created by overlaying the orange fluorescent images of the same view before (orange) and after (black) LEAP processing. This combined image shows only CEM cells and confirms that very few of the targeted CEM cells remained attached (Panel 4, Region 4). The majority of the targeted cells has detached, but still remains visible (Panel 4, Region 5). This plating density resulted in greater than 50% cell recovery with more than 90% purity.

The recovered, purified KG-1a cells suffered no apparent damage and could be cultured further. For this application, low-level laser power (25–50%) was applied in several (3–10) repeats.

The main characteristics of all LEAP-purification experiments are summarized in Table 1.

## Optoinjection of Live Adherent Cells

Optoinjection (delivering macromolecules into cells by laser irradiation) effects after targeting and shooting at cells by LEAP have been reported by Clark et al (19). When we added fluorescent dextrans (TMR-conjugated dextran; $M_W$ = 10 kDa) into the medium prior to the ablation experiments, we observed such optoinjection effects (Figs. 2A (Panels 2, 4, 6) and 2B (Panel 2)) on untargeted cells. The cells bordering the ablated regions turned fluorescent as they took up dextran molecules, while the cells seeded at other regions of the slide chamber remained dextran-negative. This indirect optoinjection effect was strongest on cells immediately bordering the ablated regions and gradually weakened towards the slide periphery. We observed an inverse correlation between the level of indirect optoinjection and the cells' distance from the targeted areas (Fig. 2B, Panel 2, Region 1). We found indirect optoinjection affected cells in an approximately 8–12 cell diameter-wide (60–120 μm) band surrounding the targeted zone (Fig. 2B, Panel 2, Region 1).

To study direct LEAP-optoinjection of confluent/semi-confluent HeLa cells, we used the laser at 20–40% of its full power, as recommended by Clark et al. (19). We introduced fluorescent dextrans of different sizes as deliverable macromolecules into the medium before LEAP-shooting to visualize optoinjection effects and to assess the size range of optoinjectable molecules. Figure 2B (Panel 4) shows a defined square region optoinjected by fluorescent 10 kDa dextrans using the grid-pattern shooting method. We found that shooting a single shot-grid at 25–50% laser power, repeated 2–3 times with a 4-s delay time between the series, optoinjected 100% of the targeted cells with very little cell loss (Panel 4, Region1). The cells were observed to be approximately evenly fluorescent within the targeted region. The optoinjection effect was found to be more direct and localized in this approach as compared with full power shooting (used in ablation experiments) and was limited to about a 4–6 cell diameter (30–60 μm) region around the targeted area. Observing the optoin-
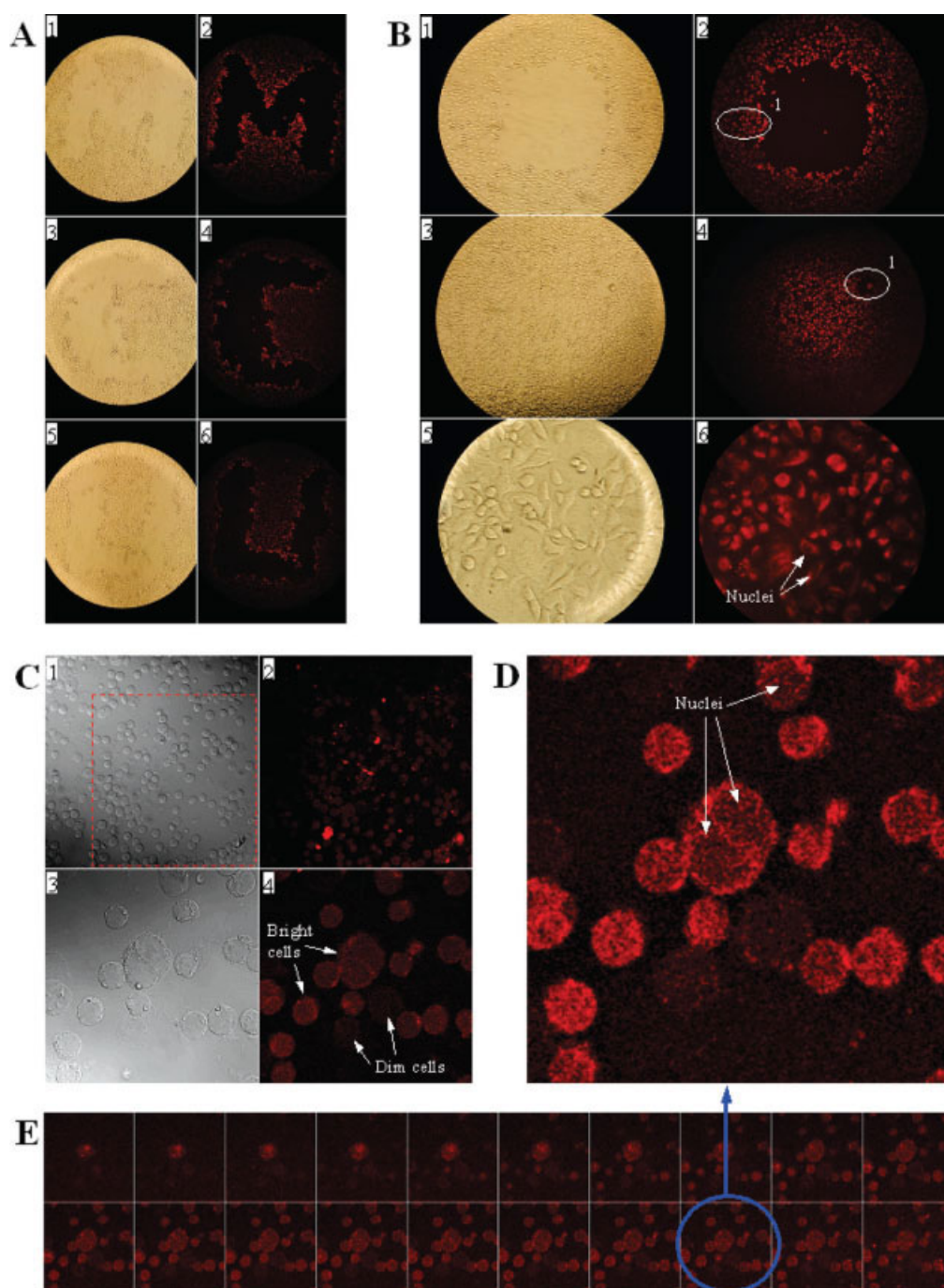
Fig. 2. Selective optoinjection of adherent cells (HeLa) and suspension cells (KG-1a). In Panels A–C brightfield (left) and darkfield (right) images of the same views were compared. **A:** Indirect optoinjection. Fluorescent dextrans were added to the medium prior to LEAP ablation of confluent cell monlayers, Panels 1–6. Untargeted cells surrounding the ablated areas were found to be optoinjected. Different geometrical shapes were targeted using the optimized protocol for controlled cell optoinjection to test injection efficacy. **B:** Optoinjection of confluent HeLa cells. Panels 1 and 2. A square pattern was shot using high laser power. The target area was ablated and indirect optoinjection occurred in the range of 8–12 cell diameters from the target area (region 1). Panels 3 and 4. A square pattern shot using low laser power. The target area was optoinjected with very few cells ablated (region 1). Panels 5 and 6. High magnification (40×) images of the optoinjected area. Most of the dextrans are observed in the cytoplasm, while the nuclei were visibly darker. **C:** Confocal images of optoinjected suspension cells. Panels 1 and 2. All cells within the targeted square area (dashed square) were optoinjected. Panels 3 and 4, higher magnification (63×) images of the optoinjected area showed a visual difference between the dextran uptake of individual cells. **D** and **E:** Optical slices of the optoinjected area. Serial images of the same view at consecutive planes confirm that the dextrans were localized within the cells, after LEAP optoinjection. A single slice was enlarged to illustrate the different concentrations of dextrans present within the cells' cytoplasm and the nucleus.

Table 2
*LEAP-Mediated Optoinjection of Adherent and Suspension Cells*

| | Percent[a] optoinjection | Delivery efficacy[b] | Indirect[c] optoinjection (μm) | Visible damage | Laser power (%) |
|---|---|---|---|---|---|
| Adherent cells | 100 | High | 30–60 | None | 25–50 |
| Suspension cells | 100 | Low | 5–30 | None | 10–20 |

[a]Percent optoinjection: percentage of optoinjected cells out of all the cells that were targeted.
[b]Delivery efficacy: relative visual brightness of fluorescent dextran-optoinjected cells.
[c]Indirect optoinjection: width of the annular zone of cells unintentionally optoinjected.

jected cells at a higher magnification (Panels 5 and 6) showed the cells to be structurally intact with a bright, dextran-positive cytoplasm and a darker, but still dextran-positive, nucleus.

In parallel experiments, we compared the optoinjectability of TMR-conjugated dextrans using the same mass/volume final concentration of 3, 10, 40, and 70 kDa dextran molecules. We observed that up to 40 kDa about the same level of cell fluorescence could be achieved. Optoinjecting HeLa cells with 70 kDa dextrans resulted in significantly lower fluorescence level than with smaller dextrans (data not shown) but this may be an artifact due to possible lower degree of TMR labeling. Larger proteins have been successfully optoinjected (19).

## Optoinjection of Live Suspension cells

Figure 2C illustrates an experiment where a square region of densely plated Kg-1a cells was optoinjected with 10 kDa fluorescent dextrans to study the effectiveness of LEAP optoinjection on temporarily semiattached suspension cells. The surrounding cells that were not targeted by the laser beam served as negative controls. Figure 2C (Panel 1) (brightfield confocal microscopy, 10× magnification) and Panel 2 (543 nm excitation) show a portion of the targeted square region (bottom, right, square area of this view) and the surrounding, untargeted cells after the shooting. Using optimized shooting conditions (single shot-grid shooting at 20% laser power; repeated twice with a 4-s delay time between the series), 100% of the targeted cells were optoinjected. The overall level of fluorescence in the targeted region was noticeably lower compared to HeLa cells. Indirect optoinjection effects were also visually weaker and less extensive than with HeLa cells; only a 1–4 cell diameter (5–30 μm) wide, faintly optoinjected region surrounded the targeted area. The fluorescent edges of the targeted area were much sharper than with adherent cell optoinjection. Looking at the cells under 63× magnification (Panels 3 and 4) confirms that the image in Panel 2 is indicative of positively optoinjected cells. These images together confirm that every targeted cell was successfully optoinjected and that the level of optoinjection varies from KG-1a cell to KG-1a cell in a much wider range (Fig. 2C, Panel 4) than with HeLa cells (Fig. 2B, Panel 6).

To confirm that the fluorescent dextran molecules were indeed inside the targeted cells after LEAP-optoinjection, several serial confocal images of the same view at consecutive vertical planes were taken (Fig. 2E). Observing the optoinjected cells at a single vertical plane, we found that most of the optoinjected molecules resided in the cells' cytoplasm with the nuclei also containing some, but much less so (Fig. 2D). Cells in both the targeted region and the surrounding areas appeared to remain morphologically intact after LEAP-optoinjection.

The main characteristics of both types of LEAP-optoinjection experiments are summarized in Table 2.

## DISCUSSION

In this study, we set out to assess the capabilities of LEAP, a new scanning cytometry technology in two fields of application: cell purification and targeted macromolecule delivery. In the purification studies, we only explored methods resulting in the immediate removal of unwanted cells. A more "patient" approach utilizing the reported apoptosis and necrosis inducing effect of LEAP irradiation (21) may lead to even better results in terms of the yield/purity ratio. However, the goal of this study was to characterize LEAP-based cell purification for immediate further cell processing (e.g. by microarray analysis).

We found that unwanted cells could be removed from attached cultures with almost "surgical" accuracy, causing minimal damage to neighboring cells within 2–3 cell diameters. Obviously, these initial studies only assessed major morphological or structural damage to the processed cells. Further studies will be necessary to study possible LEAP-processing related minor alterations in these cells' gene expression profile (GEP), proteome, and eventually the full spectrum of their cytome. If these studies confirm that LEAP does not (or only transiently) affect the majority of the untargeted cells, while accurately removes unwanted cells from confluent tissue cultures, it might prove to be a special tool in tissue engineering projects.

Another major strength of LEAP technology is the ability to deal with "problematic" cells where flow cytometry, laser capture microscopy (LCM), or magnetic bead sorting are not feasible options. Primary hepatocytes, as an example, are extremely sensitive to manipulation with conventional techniques. Maintaining structurally and functionally intact hepatocytes throughout the purification process is crucial for further analysis, culturing, and experimentation. We showed that LEAP provides the unique ability to purify these kinds of cells without trypsinization and without causing any visible damage to these fragile cells.

Processing live, suspension cells is always a challenge in scanning cytometry, since the targeted cells need to be held in the focal plane of analysis and manipulation. To

purify suspension cells by LEAP, we found that cells could be gently centrifuged to the slide/well surface and afterwards they remained in a semiattached state with no additional attachment material needed and without any apparent damage to the cells. Another observation was that targeting settled suspension cells with LEAP often resulted in these cells "bouncing" off the surface of the tissue culture well apparently unharmed rather than ablating these unwanted cells. These buoyant cells appeared in the recovered, purified cell population as contaminating cells. At the same time the high energy shooting required for ablation caused some untargeted neighboring cells to detach as well. For these reasons, we changed our strategy and utilized this "bouncing effect" of LEAP shooting (requiring less laser power) instead of aiming for ablation. We centrifuged the cell mixture onto the slide surface without causing any apparent damage to the cells and bounced off the unwanted cells from this semiattached state by LEAP shooting. We observed that many of the targeted cells still were ablated, indicating that the amount of energy required for ablation of CEM cells varies in a quite wide range. After LEAP processing, we first removed the floating cells with a very gentle wash and then recovered the purified cells using a more aggressive wash. With this approach, we achieved much higher purity (above 90% in most applications) in the recovered cell population than when we were aiming for ablation of the contaminating cells alone. In many applications where the targeted cells are highly LEAP-irradiation sensitive, ablation might be the better approach for purification. In other cases—as in our suspension cell model— bouncing off contaminating cells using sublethal laser power may be more advantageous, especially since using less power allows for higher cell plating density that ultimately results in less time needed to purify a given number of cells. This aspect may be important in studies where a large number of purified cells are required (e.g. microarray analysis).

We established optimal cell plating densities needed for a given experiment based on the ratio of contaminating cells, the required end-purity, and the affordable cell loss. We showed that when recovery of most purified cells is an important issue as from a small sample, it is possible to achieve above 95% purity and above 80% cell recovery with LEAP even from a 50% cell mixture. This requires low density cell plating that ultimately results in slower cell processing, but with small cell samples this is usually not an issue since the process still only takes a few minutes after the initial setup. In large cell samples where 30–50% cell loss is not a problem, the cells can be plated denser significantly increasing the processing speed and still maintaining above 90% purity. We observed no apparent damage to the purified cells with either method.

We report here an indirect optoinjection effect at the edges of the ablation zone in confluent adherent cultures that might be a sign of altered membrane and other functions in the purified cells. However, these effects are likely to be transient, lasting only for a few seconds since these cells did not show any signs of "leakiness" or morphologi-

cal damage a few minutes after the indirect optoinjection as determined by confocal, brightfield, and fluorescent microscopy. The width of this indirectly optoinjected zone appeared to depend on the cell type and the laser power used in the experiment. As discussed earlier, further studies will be needed to elucidate these effects on different levels of the cell's cytome.

LEAP-mediated optoinjection is a novel tool for targeted macromolecule delivery. We studied optoinjection effects adding fluorescent dextrans of different sizes as deliverable macromolecules into the medium before LEAP shooting to visualize optoinjection effects. We found that optoinjection works with all cell types we studied (adherent and suspension cells) with no exception. It is even more promising that for every cell type we studied, it could be optimized to achieve literally 100% optoinjection of the targeted cells. When low laser power was used, we found no apparent morphological damage to any of the cell types. Optimized conditions, the concentration, size, and nature of macromolecules deliverable, and the optoinjection effects on cells close to the targets varied according to the different applications used.

It should be noted that adherent cells are easier to manipulate with LEAP, since it does not require extra effort to keep them in the focal plane. The optoinjection effect appeared to be more diffuse on adherent cells than on suspension cells with indirect optoinjection visibly affecting cells up to 4–6 cell diameters away from the targeted zone. This indirect optoinjection effect as well as the amount of macromolecules delivered to the targeted cells (measured by the visible level of fluorescence) directly correlated with the laser power and the number of pulses applied. Higher laser power applied in fewer pulses and lower power applied in more pulses resulted in similar levels of fluorescence. Logically, the more sum energy delivered to the cells resulted in higher fluorescence levels and a wider zone of indirect optoinjection—up to a certain point. Both of these effects seemed to reach a plateau at a certain level, depending on the cell type. Delivering more energy above this plateau (by raising laser power or applying more pulses per cell) did not raise the level of fluorescence significantly, but caused visible cell damage. On the basis of these observations, we could optimize LEAP-shooting conditions for each cell type and application maximizing optoinjection effects without causing any visible damage to the targeted cells.

Gently centrifuged suspension cells could be optoinjected similarly to attached cells; the laser energy required for optoinjection did not remove the cells from the slide surface. The level of fluorescence was found to be higher even within the targeted region when we optoinjected adherent cells than with suspension cells. A possible reason could be that adherent cells are flat, all of them lying exactly in the focal plane, while suspension cells even in their semiattached state keep a certain vertical diameter depending on their size that causes them to stick out of the slide surface unevenly. Alternatively, flat cell membrane may be more susceptible to optoinjection than spherical shaped. This could also explain the fact that we

found much less indirect optoinjection effect only (1–4 cell diameter wide zone) with suspension cells than with adherent cells (4–6 cell diameter wide zone).

Confocal microscopy results confirmed that the fluorescent dextran molecules were indeed inside the cells after optoinjection. Most of the optoinjected molecules were found in the cells' cytoplasm with the nuclei remaining relatively negative although, in some cases, visibly optoinjected. This analysis also confirmed that optoinjection did not cause any apparent alteration in cellular morphology.

The maximum size of optoinjectable macromolecules and the efficacy of optoinjection for macromolecules with different size and chemical structure still need to be determined. We observed very similar results with 3–40 kDa dextrans and significantly reduced ($\sim$50%) fluorescence of optoinjected cells when using 70 kDa dextrans. These observations might mean that the limits of the underlying mechanism are not much above the size of a 70 kDa dextran molecule. The limiting size of optoinjected molecules remains to be fully determined.

Laser irradiation mediated cell membrane permeability changes and optoinjection effects have been reported by several studies, but the mechanism of optoinjection is unknown (19,25,26). It is not likely that the laser directly punches holes into the membrane of the targeted cell, because this theory could not explain the indirect optoinjection phenomenon we observed in this study. Shock waves created in the culture medium by laser shooting might contribute to the effects (27), but they alone do not have enough energy to achieve macromolecule delivery through the cell membrane (19). The distance dependent diffuse optoinjection phenomenon and the results with different laser energy/pulse number combinations suggest that the level of optoinjection depends on the sum energy communicated to the cells. Here we are reporting the direct experimental results, and do not attempt the very complicated and extensive experiments required to elucidate the molecular-level mechanisms of laser optoinjection, which are not well understood at this time. On the basis of these observations, we propose the following possible mechanistic theory, which will require further testing beyond the scope of this paper.

Laser energy is absorbed by different molecules in the medium around the cells, in the cell membrane, and inside the cells warming up the cells in the targeted area. This heating effect of laser irradiation on cells and tissues is well characterized and used in therapeutic applications (28–30). As a result of warming up beyond a certain threshold, the cell membrane goes through a phase change becoming more liquid-like than gel-like (31–33). The uneven warming and the low energy shockwaves caused by the pulsing laser (27) generate waves in the fluid cell membrane. These waves may result in opening transient holes in the cell membrane or in transiently opening and enlarging existing pores and channels. If the sum laser energy is large enough to create membrane ruptures beyond the cells healing capabilities or even cause the cytoplasm to explode (increase its volume beyond the membranes flexibility), the end

result will be ablation or permanent damage. If the sum energy is not enough for the aforementioned effects, but enough to cause transient membrane disturbances, the end result will be sum energy dependent optoinjection. If the sum absorbed energy stays below a certain threshold the cell membrane will remain intact and no optoinjection will occur. Further experiments will be needed to elucidate the underlying mechanism(s) for optoinjection.

In summary, LEAP offers a novel approach in analyzing, purifying, and manipulating live cells. For analysis, the LEAP system functions as a scanning cytometer with cell sorting and optoinjection capabilities. It is a combined fluorescence imaging microscope linked to a computer, enabling the user to observe and record the processed sample before, during, and after different LEAP applications, without moving it in and out of the system. Real-time decisions can be made based on multicolor images and this decision-making process can be automated by setting the hardware and software parameters appropriately. With these analytical capabilities, LEAP promises to offer high-throughput cell processing based on high-content analysis. For cell purification, LEAP combines advantages of flow cytometry-cell sorting and LCM in a unique fashion. Practical applications for LEAP-mediated cell purification can range from traditional cell sorting all the way to tissue surgery. LEAP might become especially useful in areas where other sorting methods are seriously challenged as in purifying large numbers of live, adherent cells; very small samples of live, suspension cells; live cells that are highly sensitive to traditional processing; and live processing of biohazardous cells. Optoinjection is an exciting capability LEAP offers to the fields of both basic research and applied sciences. The virtually 100% efficacy, highly accurate selectivity, and very low toxicity/cell damage we observed are unmatched features by any other existing method for macromolecule delivery into cells. Optoinjection could be used in a wide variety of applications such as cloning, cell tracking, single cell targeted drug delivery, antisense-RNA and siRNA delivery to selected cells—applications now in progress in our laboratory.

## LITERATURE CITED

1. Kamentsky LA. Laser scanning cytometry. Methods Cell Biol 2001;63: 51–87.
2. Luther E, Kamentsky L, Henriksen M, Holden E. Next generation laser scanning cytometry. In: Darzynkiewicz Z, Roederer M, Tanke H, editors. Methods in Cell Biology, Vol 75. Amsterdam: Elsevier; 2004. p 185–218.

3. Kamentsky LA, Kamentsky LD. Microscope-based multiparameter laser scanning cytometer yielding data comparable to flow cytometry data. Cytometry 1991;12:381–387.

4. Price J, Gough DA. Operator independent image cytometer. US Patent No. 5,548,661, 1996.

5. Price J, Gough DA. Autofocus system for scanning microscopy. US Patent No. 5,790,710, 1998.

6. Abraham VC, Taylor DL, Haskins JR. High content screening applied to large-scale cell biology. Trends Biotechnol 2004;22:15–22.

7. Bedner E, Burfeind P, Gorczyca W, Melamed MR, Darzynkiewicz Z. Laser scanning cytometry distinguishes lymphocytes, monocytes, and granulocytes by differences in their chromatin structure. Cytometry 1997;29:191–196.

8. Bedner E, Ruan Q, Chen S, Kamentsky LA, Darzynkiewicz Z. Multiparameter analysis of progeny of individual cells by laser scanning cytometry. Cytometry 2000;40:271–279.

9. Clatch RJ, Walloch JL, Zutter MM, Kamentsky LA. Immunophenotypic analysis of hematologic malignancy by laser scanning cytometry. Am J Clin Pathol 1996;105:744–755.

10. Clatch RJ, Foreman JR, Walloch JL. Simplified immunophenotypic analysis by laser scanning cytometry. Cytometry 1998;34:3–16.

11. Gerstner A, Laffers W, Bootz F, Tarnok A. Immunophenotyping of peripheral blood leukocytes by laser scanning cytometry. J Immunol Methods 2000;246:175–185.

12. Gerstner AO, Lenz D, Laffers W, Hoffman RA, Steinbrecher M, Bootz F, Tarnok A. Near-infrared dyes for six-color immunophenotyping by laser scanning cytometry. Cytometry 2002;48:115–123.

13. Gorczyca W, Darzynkiewicz Z, Melamed MR. Laser scanning cytometry in pathology of solid tumors. A review. Acta Cytol 1997;41:98–108.

14. Gorczyca W, Deptala A, Bedner E, Li X, Melamed MR, Darzynkiewicz Z. Analysis of human tumors by laser scanning cytometry. Methods Cell Biol 2001;64:421–443.

15. Lenz D, Gerstner AO, Laffers W, SteinBrecher M, Bootz F, Tarnok A, editors. Six and More Color Immunophenotyping on the Slide by Laser Scanning Cytometry (LSC). Proc SPIE 2003; 4962. pp 364–374.

16. Tarnok A, Gerstner AO. Clinical applications of laser scanning cytometry. Cytometry 2002;50:133–143.

17. Bonner RF, Emmert-Buck M, Cole K, Pohida T, Chuaqui R, Goldstein S, Liotta LA. Laser capture microdissection: molecular analysis of tissue. Science 1997;278:1481–1483.

18. Buican T, Neagley DL, Morrison WC, Upham BD. Optical trapping, cell manipulation, and robotics. In: Salzman GC, editor. Proc SPIE 1989; 1063: p 190.

19. Clark IB, Hanania EG, Stevens J, Gallina M, Fieck A, Brandes R, Palsson BO, Koller MR. Optoinjection for efficient delivery of a broad range of compounds and macromolecules into diverse cell types. J Biomed Optics 2006;11(1):014034-1–014034-8.

20. Koller M, Hanania EG, Eisfeld TM, Palsson BO. Optoinjection methods. US Patent No. 6,753,161; 2004.

21. Koller MR, Hanania EG, Stevens J, Eisfeld TM, Sasaki GC, Fieck A, Palsson BO. High-throughput laser-mediated in situ cell purification with high purity and yield. Cytometry 2004;61A:153–161.

22. Palsson B, Koller M, Eisfeld T. Method and apparatus for selectively targeting specific cells within a mixed cell population. US Patent No. 6,534,308; 2003.

23. Zaher H, Fernandez-Salguero PM, Letterio J, Sheikh MS, Fornace AJ Jr, Roberts AB, Gonzalez FJ. The involvement of aryl hydrocarbon receptor in the activation of transforming growth factor-beta and apoptosis. Mol Pharmacol 1998;54:313–321.

24. Huang G, Elferink CJ. Multiple mechanisms are involved in Ah receptor-mediated cell cycle arrest. Mol Pharmacol 2005;67:88–96.

25. Mohanty SK, Sharma M, Gupta PK. Laser-assisted microinjection into targeted animal cells. Biotechnol Letters 2003;25:895–899.

26. Umebayashi Y, Miyamoto Y, Wakita M, Kobayashi A, Nishisaka T. Elevation of plasma membrane permeability on laser irradiation of extracellular latex particles. J Biochem 2003;134:219–224.

27. Soughayer JS, Krasieva T, Jacobson SC, Ramsey JM, Tromberg BJ, Allbritton NL. Characterization of cellular optoporation with distance. Anal Chem 2000;72:1342–1347.

28. Fatemi A, Weiss MA, Weiss RA. Short-term histologic effects of nonablative resurfacing: Results with a dynamically cooled millisecond-domain 1320 nm Nd: YAG laser. Dermatol Surg 2002;28:172–176.

29. Gaon MD, Ho KH, Wong BJ. Measurement of the elastic modulus of porcine septal cartilage specimens following Nd: YAG laser treatment. Lasers Med Sci 2003;18:148–153.

30. He X, Bischof JC. Quantification of temperature and injury response in thermal therapy and cryosurgery. Crit Rev Biomed Eng 2003;31:355–422.

31. Bloom M, Evans E, Mouritsen OG. Physical properties of the fluid lipid-bilayer component of cell membranes: A perspective. Q Rev Biophys 1991;24:293–397.

32. Hyslop PA, Kuhn CE, Sauerheber RD. Temperature optimum of insulin-stimulated 2-deoxy-D-glucose uptake in rat adipocytes. Correlation of cellular transport with membrane spin-label and fluorescence-label data. Biochem J 1984;218:29–36.

33. Moriyama-Gonda N, Igawa M, Shiina H, Wada Y. Heat-induced membrane damage combined with adriamycin on prostate carcinoma PC-3 cells: Correlation of cytotoxicity, permeability and P-glycoprotein or metallothionein expression. Br J Urol 1998;82:552–559.